Continuous lipase-catalyzed production of pseudo-ceramides in a packed-bed bioreactor

Florian Le Joubioux, Nicolas Bridiau, Mehdi Sanekli, Marianne Graber, Thierry Maugard

Continuous lipase-catalyzed production of pseudo-ceramides in a packed-bed bioreactor

Florian Le Joubioux, Nicolas Bridiau*, Mehdi Sanekli, Marianne Graber, Thierry Maugard

Equipe Approches Moléculaires, Environnement-Santé, UMR 7266 CNRS-ULR, LIENSs, Université de La Rochelle, Avenue Michel Crépeau, 17042 La Rochelle, France.

Author for correspondence (Fax: +33 546458265; E-mail: nicolas.bridiau@univ-lr.fr)

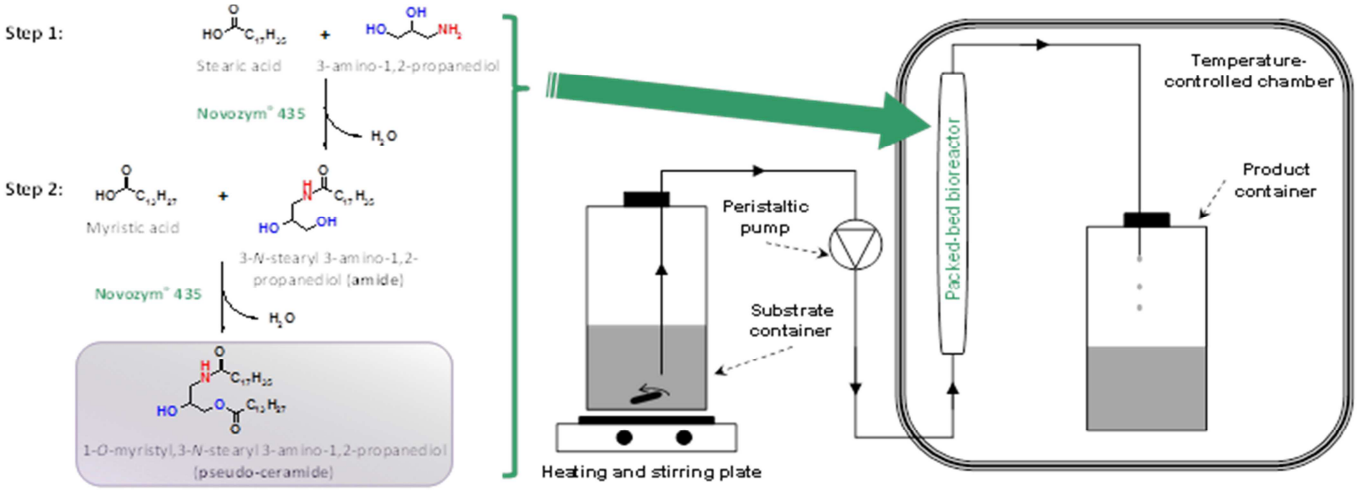
Step 1:
Stearic acid
3-amino-1,2-propanediol
Novozym® 435
H_2O
Step 2:
Myristic acid
3-N-stearyl 3-amino-1,2-propanediol (amide)
Novozym® 435
H_2O
1-O-myristyl,3-N-stearyl 3-amino-1,2-propanediol (pseudo-ceramide)
Temperature-controlled chamber
Packed-bed bioreactor
Product container
Peristaltic pump
Substrate container
Heating and stirring plate

11
12

Abstract

Ceramides are spingolipid compounds that are very attractive as active components in both the pharmaceutical and the cosmetic industries. In this study, the synthesis of ceramide analogs, the so-called pseudo-ceramides, was carried out using for the first time a two-step continuous enzymatic process with immobilized *Candida antarcti*ca lipase B (Novozym® 435) in a packed-bed bioreactor. The first step involved the selective *N*-acylation of 3-amino-1,2-propanediol using stearic acid as the first acyl donor (i). This was followed by the selective *O*-acylation of the *N*-stearyl 3-amino-1,2-propanediol synthesized in the first step, with myristic acid as the second acyl donor, to produce a *N*,*O*-diacyl 3-amino-1,2-propanediol-type pseudo-ceramide, namely 1-*O*-myristyl,3-*N*-stearyl 3-amino-1,2-propanediol (ii). The process was first optimized by evaluating the influences of three factors: feed flow rate, quantity of biocatalyst and substrate concentration. Under optimal conditions an amide synthesis yield of 92% and a satisfying production rate of almost 3.15 mmol h^{-1} $g_{biocatalyst}^{-1}$ (1128 mg h^{-1} $g_{biocatalyst}^{-1}$) were obtained. The second step, *N*-acyl 3-amino-1,2-propanediol *O*-acylation, was similarly optimized and in addition the effect of the substrate molar ratio was studied. Thus, an optimal pseudo-ceramide synthesis yield of 54% and a production rate of 0.46 mmol h^{-1} $g_{biocatalyst}^{-1}$ (261 mg h^{-1} $g_{biocatalyst}^{-1}$) were reached at a 1:3 ratio of amide to fatty acid. In addition, it was demonstrated that this two-step process has great potential for the production of *N*,*O*-diacyl 3-amino-1,2-propanediol-type pseudo-ceramides on an industrial scale. It was shown in particular that Novozym® 435 could be used for more than 3 weeks without a drop in the yield during the first step of 3-amino-1,2-propanediol *N*-acylation, proving that this biocatalyst is very stable under these operational conditions. This factor would greatly reduce the need for biocatalyst replacement and significantly lower the associated cost.

Keywords: pseudo-ceramide, biocatalysis, lipase, continuous bioprocess, packed-bed bioreactor

1. Introduction

Ceramides are natural compounds derived from the *N*-acylation of sphingosine and are key intermediates in the biosynthesis of all complex sphingolipids. Like their synthetic analogs, they have been widely used in the cosmetic and pharmaceutical industries. Indeed, due to their major role in preserving the water-retaining properties of the epidermis [1], ceramides have a wide range of commercial applications in the cosmetic industry as active ingredients included in hair and skin care products. Moreover, ceramides can be used as active components in dermatological therapy: they are effective in restoring the water content of dry skin and in relieving atopic eczema [2]. In addition, it has been demonstrated that they have commercial applications in the pharmaceutical industry as potential anti-viral or anti-tumor drugs [3, 4] and anti-oxidant stabilizers [5].

As a result of these numerous commercial applications, there is a growing interest in the development and optimization of new processes for ceramide synthesis. Ceramide synthesis is usually performed by acylation of the amino group of a sphingosine, a sphinganine or their derivatives [6–8]. However, due to the high cost of sphingoid bases, whose chemical synthesis is complex, other approaches have been developed to synthesize ceramide analogs, called pseudo-ceramides, by the selective acylation of multifunctional compounds like amino-alcohols. All these compounds are presently synthesized by chemical procedures which require fastidious steps of alcohol group protection and deprotection for the control of chemoselectivity, regioselectivity and stereoselectivity [6–10]. Moreover, these procedures often require high temperatures that may preclude the use of fragile molecules and may cause coloration of the end products. In addition, the coproduction of salts and the use of toxic solvents (dimethylformamide, methanol, etc.) that must be eliminated at the end of the reaction tend to increase the cost of the processes.

In order to overcome these disadvantages, several studies focused on developing enzymatic syntheses of pseudo-ceramides through immobilized lipase-catalyzed acylation or transacylation reactions carried out in an organic solvent or in a solvent-free system [11–13]. Indeed, using lipases (E.C. 3.1.1.3) in the process can be both more effective, due to a higher selectivity, and more eco-compatible, due to the limited number of steps required for the synthesis [14–18]. Lipase-catalyzed acylation in organic media provides several advantages such as shifting the thermodynamic equilibrium toward synthesis rather than hydrolysis, increasing the solubility of non-polar substrates like fatty acids, eliminating side reactions, making enzyme recovery easier and increasing enzyme thermostability [19].

Various studies have been devoted to the lipase-catalyzed acylation of multi-functional molecules similar to the substrates used as precursors for the synthesis of pseudo-ceramides. These molecules have both amino and alcohol groups, such as ethanolamine, diethanolamine, 2-amino-1-butanol, 6-amino-1-hexanol, serine and other amino-alcohols of variable carbon chain length [20–28]. In such reactions, it has been shown that the lipases used can catalyze the chemoselective acylation of these substrates in a highly efficient and chemoselective manner. Some of these studies have already demonstrated the feasibility of selectively synthesizing pseudo-ceramide-type compounds using heterogeneous solvent-free media in a batch bioreactor, with productivity close to 15 $g_{pseudo\text{-}ceramide}\ g_{biocatalyst}^{-1}$ [12, 26]. Based on these studies, lipases seem to be the ideal biocatalysts for the synthesis of pseudo-ceramide compounds.

On the other hand, despite the many synthetic processes that have already been developed, also in batch reactors [6-13, 29], ceramides are still not easy to produce for industrial applications. The price of the cheapest synthetic ceramide is close to 2000 €/kg, and ceramides with a fatty acid composition similar to that found in the skin cost several hundred thousand €/kg. So, it would be extremely beneficial to develop an alternative cost-efficient

method to produce this valuable product with a high yield and productivity. In recent years, the use of continuous-flow technology has become an innovative, promising and attractive alternative for the highly selective production of pure chemical compounds with a good level of productivity. Packed-bed bioreactors are the most frequently used and the best continuous production systems. They offer several advantages over a batch reactor: they are easy to use, can be controlled and operated automatically, they reduce operating costs, provide a better control of the operating conditions and products, leading to a significant enhancement in the productivity of the biocatalyst and an improvement in quality (less secondary products) and yield [30, 31]. Such systems have a low reactor volume due to the high enzyme/substrate ratio maintained in the catalytic bed. In addition, the enzyme/substrate ratio is higher in packed-bed bioreactors than in conventional batch bioreactors, thus shortening the reaction time and potentially limiting side reactions, thereby improving selectivity.

Starting from this overview, the aim of our work was to develop for the first time a continuous process for the efficient enzymatic production of 1-*O*,3-*N*-diacyl 3-amino-1,2-propanediol-type pseudo-ceramides. These diacylated derivatives of 3-amino-1,2-propanediol have been considered in various studies as pseudo-ceramides for two reasons: i) their structure includes a polar head, two lipophilic carbon chains and an amide bond, and is thus very close to natural ceramide structure; ii) they have been demonstrated to have restructuring effects very similar to those of natural ceramides at the level of the uppermost skin layer, the so-called *stratum corneum* [12, 26, 32].

The process developed in this work was performed using a packed-bed bioreactor containing immobilized *Candida antarctica* lipase B (Novozym® 435). In order to control the chemoselectivity of the reaction, the process was divided into two steps (scheme 1): *N*-stearyl 3-amino-1,2-propanediol **3a** (amide) was obtained in the first step from the *N*-acylation of 3-amino-1,2-propanediol **1** using stearic acid **2a** as a first acyl donor. In the second step, 1-*O*-

myristyl,3-*N*-stearyl 3-amino-1,2-propanediols **4** (pseudo-ceramide) was produced from the *O*-acylation of the *N*-stearyl 3-amino-1,2-propanediol **3a** (amide) produced in the first step using myristic acid **2b** as a second acyl donor.

Scheme 1.

2. Material and methods

2.1. Enzymes and chemicals

Novozym® 435 (immobilized *Candida antarctica* lipase B) was kindly provided by Novozymes A/S, Bagsvaerd, Denmark. (±)-3-amino-1,2-propanediol (97%), lauric acid (≥99%), stearic acid (95%), linoleic acid (≥99%) and *tert*-amyl alcohol (99%) were purchased from Sigma Aldrich (St Louis, USA) while myristic acid (≥98%) and oleic acid (97%) were purchased from Fluka (St Quentin-Fallavier, Switzerland). All chemicals were dried over molecular sieves. Pure water was obtained via a Milli-Q system (Millipore, France). Acetonitrile, methanol, *n*-hexane and chloroform were purchased from Carlo ERBA (Val-de-Reuil, France).

2.2. Continuous process using a packed-bed bioreactor system for the Novozym® 435-catalyzed synthesis of 1-O,3-N-diacyl 3-amino-1,2-propanediol-type pseudo-ceramides

2.2.1. Packed-bed bioreactor system

Fig. 1 schematically shows the packed-bed bioreactor system used for the continuous two-step enzymatic synthesis of 1-*O*,3-*N*-diacyl 3-amino-1,2-propanediol-type pseudo-ceramides catalyzed by immobilized *Candida antarctica* lipase B (Novozym® 435) (scheme 1). For each step, the reaction mixture (substrates and solvent) was first homogenized for 15 min at 55°C

while stirring at 250 rpm. The process was then started by percolating the reaction mixture into a column packed with Novozym® 435 by means of a peristaltic pump (Minipuls Evolution Peristaltic Pump from Gilson Inc., USA). Several stainless steel columns of variable length and an inner diameter of 5 mm were used at the laboratory scale, while one 125 mm long column with a 10 mm inner diameter and a second that was 5 mm in length with an inner diameter of 50 mm were used to scale-up the reactor design. Throughout the process, the reaction medium leaving the bioreactor was continuously pooled into a product container which, together with the column packed with Novozym® 435, was placed in a temperature-controlled chamber at 55°C to promote the synthesis reaction and ensure the solubility of the acylated products. Each step was carried out until the substrate container was empty, indicating the end of the process. The concentration of the remaining substrates and acylated products in the product container were then determined by LC/MS-ESI analysis.

Fig. 1

2.2.2. First step: N-acylation of 3-amino-1,2-propanediol

In the first step, the reaction mixture contained 3-amino-1,2-propanediol **1**, a fatty acid (stearic acid **2a**, myristic acid **2b**, lauric acid **2c**, oleic acid **2d** or linoleic acid **2e**), which was used as an acyl donor, and a *tert*-amyl alcohol/*n*-hexane (50:50 v/v) mixture used as the reaction solvent.

2.2.3. Second step: O-acylation of N-acyl 3-amino-1,2-propanediol

In the second step, the reaction mixture contained the *N*-stearyl 3-amino-1,2-propanediol **3a** produced during the first step, myristic acid **2b**, which was used as an acyl donor and a *tert*-amyl alcohol/*n*-hexane (50:50 v/v) mixture used as the reaction solvent.

2.3. HPLC/MS analysis

To monitor the reaction, a 500 µl sample was taken from the product container when the continuous process was complete, after 1 h of reaction. The study of the operational stability of Novozym® 435 in the continuous packed-bed bioreactor was carried out in a slightly different manner: 500 µl samples were taken from the packed-bed output at different times over a 3-week period. In each case, 500 µl of a methanol/chloroform (50:50 v/v) mixture were added to each sample in order to homogenize the reaction medium at room temperature. Structural and quantitative analyses of the reaction products were then conducted on these samples using a LC/MS-ES system from Agilent (1100 LC/MSD Trap mass spectrometer VL) with a C18 Prontosil 120-5-C18-AQ reversed-phase column (250×4 mm, 5 µm; Bischoff Chromatography, Germany). The elution of the reaction samples was carried out at room temperature and at a flow rate of 1 ml min^{-1} using a gradient that was derived from two eluent mixtures (Table 1). The products were detected and quantified by differential refractometry and UV detection at 210 nm. Quantification was performed against external calibration lines prepared using the appropriate acylated products as standards. These standards were synthesized using operating conditions in which only a specific standard could be formed using a given acyl donor, then purified and structurally characterized. Low-resolution mass spectral analyses were obtained by electrospray in the positive detection mode. Nitrogen was used as the drying gas at 15 l min^{-1}, 350 °C and at a nebulizer pressure of 4 bars. The scan range was 50–1000 *m/z* using five averages and 13,000 *m/z* per second resolution. The capillary voltage was 4000 V. Processing was done offline using HP Chemstation software.

Table 1

2.4. Purification and characterization of reaction products

The reaction products were purified with a preparative HPLC system from Agilent (1200 LC/MSD) using a ProntoPrep C18 reversed-phase column (250×20 mm, 10 µm; Bischoff

Chromatography, Germany) eluted according to the gradient given in Table 1, at room temperature and at a flow rate of 5 ml min^{-1}. The purified products were then characterized by ^1H NMR and infrared (IR) spectroscopy. The ^1H NMR chemical shift values were recorded on a JEOL-JNM LA400 spectrometer (400 MHz), with tetramethylsilane as an internal reference. The samples were studied as solutions in $CDCl_3$. IR spectra were recorded from 400 to 4000 cm^{-1} with a resolution of 4 cm^{-1} using a 100 ATR spectrometer (Perkin-Elmer, United States).

2.4.1. N-stearyl 3-amino-1,2-propanediol ***3a***

m/z (LR-ESI$^+$) $C_{21}H_{44}NO_3$ (M + H^+), found: 358.2, calculated for: 358.58. IR ν_{max} (cm^{-1}): 3312 (O-H, alcohol and N-H, amide), 2800-3000 (CH of stearyl chain), 1633 (C=O, amide), 1544 (N-H, amide). ^1H NMR (400 MHz, $CDCl_3$, δ ppm): δ 0.88 (t, 3H, *J*= 6.03Hz, -CH_2-C$\underline{H}_3$), 1.25 (m, 28H, -CH_2- of stearyl chain), 1.63 (m, 2H, -C$\underline{H}_2$-CH_2-CO-NH- of stearyl chain), 2.21 (t, 2H, *J*= 7.57Hz, -CH_2-C$\underline{H}_2$-CO-NH- of stearyl chain), 3.42 (m, 2H, –CH-C$\underline{H}_2$-OH), 3.54 (m, 2H,–CH-C$\underline{H}_2$-NH-), 3.75 (m, 1H, -CH-), 5.84 (s, 1H, -NH-).

2.4.2. N-myristyl 3-amino-1,2-propanediol ***3b***

m/z (LR-ESI$^+$) $C_{17}H_{36}NO_3$ (M + H^+), found: 302.1, calculated for: 302.47. IR ν_{max} (cm^{-1}): 3298 (O-H, alcohol and N-H, amide), 2800-3000 (CH of myristyl chain), 1634 (C=O, amide), 1546 (N-H, amide). ^1H NMR (400 MHz, $CDCl_3$, δ ppm): δ 0.88 (t, 3H, *J*= 6.55Hz, -CH_2-C$\underline{H}_3$), 1.25 (m, 20H, -CH_2- of myristyl chain), 1.63 (m, 2H, -C$\underline{H}_2$-CH_2-CO-NH- of myristyl chain), 2.21 (t, 2H, *J*= 8Hz, -CH_2-C$\underline{H}_2$-CO-NH- of myristyl chain), 3.42 (m, 2H, –CH-C$\underline{H}_2$-OH), 3.56 (m, 2H,–CH-C$\underline{H}_2$-NH-), 3.76 (m, 1H, -CH-), 5.88 (s, 1H, -NH-).

2.4.3. N-lauryl 3-amino-1,2-propanediol ***3c***

m/z (LR-ESI$^+$) $C_{15}H_{32}NO_3$ (M + H^+), found: 274.2, calculated for: 274.43. IR ν_{max} (cm^{-1}): 3307 (O-H, alcohol and N-H, amide), 2800-3000 (CH of lauryl chain), 1631 (C=O, amide), 1545 (N-H, amide). ^1H NMR (400 MHz, $CDCl_3$, δ ppm): δ 0.88 (t, 3H, *J*= 7Hz, -CH_2-C$\underline{H}_3$), 1.26 (m, 16H, -CH_2- of lauryl

chain), 1.62 (m, 2H, -C$\underline{H_2}$-CH_2-CO-NH- of lauryl chain), 2.23 (t, 2H, *J*= 7.23Hz, -CH_2-C$\underline{H_2}$-CO-NH- of lauryl chain), 3.43 (m, 2H, –CH-C$\underline{H_2}$-OH), 3.56 (m, 2H,–CH-C$\underline{H_2}$-NH-), 3.76 (m, 1H, -CH-), 5.92 (s, 1H, -NH-).

2.4.4. N-oleyl 3-amino-1,2-propanediol ***3d***

m/z (LR-ESI$^+$) $C_{21}H_{42}NO_3$ (M + H^+), found: 356.2, calculated for: 356.57. IR ν_{max} (cm^{-1}): 3342 (O-H, alcohol and N-H, amide), 2800-3000 (CH of oleyl chain), 1632(C=O, amide), 1546 (N-H, amide). ^{1}H NMR (400 MHz, $CDCl_3$, δ ppm): δ 0.88 (t, 3H, *J*= 6.55Hz, -CH_2-C$\underline{H_3}$), 1.27 (m, 12H, CH-CH_2-$\underline{CH_2}$-$\underline{CH_2}$-$\underline{CH_2}$-$\underline{CH_2}$-$\underline{CH_2}$-CH_3 of oleyl chain), 1.31 (m, 8H, CH-CH_2-$\underline{CH_2}$-$\underline{CH_2}$-$\underline{CH_2}$-$\underline{CH_2}$-CH_2-CH_2-CO-NH of oleyl chain), 1.64 (m, 2H, -C$\underline{H_2}$-CH_2-CO-NH- of oleyl chain), 2.01 (m, 4H, -$\underline{CH_2}$-CH=CH-$\underline{CH_2}$- of oleyl chain), 2.22 (t, 2H, *J*= 7.24Hz, -CH_2-C$\underline{H_2}$-CO-NH- of oleyl chain), 3.41 (m, 2H, –CH-C$\underline{H_2}$-OH), 3.53 (m, 2H,–CH-C$\underline{H_2}$-NH-), 3.72 (m, 1H, -CH-), 5.34 (m, 2H, -CH_2-$\underline{CH=CH}$-CH_2- of oleyl chain), 5.94 (s, 1H, -NH-).

2.4.5. N-linoleyl 3-amino-1,2-propanediol ***3e***

m/z (LR-ESI$^+$) $C_{21}H_{40}NO_3$ (M + H^+), found: 354.1, calculated for: 354.56. IR ν_{max} (cm^{-1}): 3303 (O-H, alcohol and N-H, amide), 2800-3000 (CH of linoleyl chain), 1634 (C=O, amide), 1548 (N-H, amide).

2.4.6. 1-O-myristyl,3-N-stearyl 3-amino-1,2-propanediol ***4***

m/z (LR-ESI$^+$) $C_{35}H_{70}NO_4Na$ (M + Na^+), found: 590.2, calculated for: 590.94. IR ν_{max} (cm^{-1}): 3651 (O-H, alcohol), 3200-3400 (O-H, alcohol and N-H, amide), 2800-3000 (CH of stearyl and myristyl chains), 1720 (C=O, ester), 1650 (C=O, amide), 1546 (N-H, amide). ^{1}H NMR (400 MHz, $CDCl_3$, δ ppm): δ 0.88 (t, 6H, *J*= 6.3Hz, 2x -CH_2-C$\underline{H_3}$), 1.25 (m, 48H, -CH_2- of stearyl and myristyl chains), 1.62 (m, 4H, 2x -C$\underline{H_2}$-CH_2-CO- of stearyl and myristyl chains), 2.21 (t, 2H, *J*= 7.11Hz, -CH_2-C$\underline{H_2}$-CO-O- of myristyl chain), 2.34 (t, 2H, *J*= 7.78Hz, -CH_2-C$\underline{H_2}$-CO-NH- of stearyl chain), 3.53 (dd, 1H, *J*= 4.88Hz, *J*= 14.15Hz, –CH-C$\underline{H_2}$-NH-), 3.56 (dd, 1H, *J*= 4.88Hz, *J*= 14.15Hz, –CH-C$\underline{H_2}$-NH-), 3.94

(m, 1H, -CH-), 4.05 (dd, 1H, *J*= 5.49Hz, *J*= 10.98Hz, –CH-C$\underline{H_2}$-O-), 4.15 (dd, 1H, *J*= 5.12Hz, *J*= 11.46Hz, –CH-C$\underline{H_2}$-O-), 5.95 (t, 1H, *J*= 5.2Hz, -NH-).

3. Results and discussion

The continuous enzymatic synthesis of 1-*O*,3-*N*-diacyl 3-amino-1,2-propanediol-type pseudo-ceramides catalyzed by immobilized *Candida antarctica* lipase B (Novozym® 435) was conducted in a packed-bed bioreactor system (Scheme 1, Fig. 1) in two steps. *N*-acyl 3-amino-1,2-propanediol (amide) was obtained from the *N*-acylation of 3-amino-1,2-propanediol **1** in the first step (step 1). In the second step (step 2), 1-*O*,3-*N*-diacyl 3-amino-1,2-propanediol (pseudo-ceramide) was then produced from the *O*-acylation of the *N*-acyl 3-amino-1,2-propanediol (amide) synthesized in step 1. In order to promote both the synthesis and the solubility of the products, all the reactions were carried out at 55°C.

A *tert*-amyl alcohol/*n*-hexane mixture (50:50 v/v) was chosen as the reaction solvent on the basis of previous work that demonstrated the capacity of these two solvents to promote the selective Novozym® 435-catalyzed synthesis of amide and amido-ester products starting from various amino-alcohols as substrates [33].

Regarding the choice of the appropriate acyl donors to use at each step of the process, we decided first to base our selection on the structure of natural ceramides, which are mostly composed of long-chain saturated fatty acids. C18:0 fatty acids are indeed one of the most abundant fatty acids incorporated in the natural ceramides located in the outer layer of the skin, namely the *stratum corneum* [34–36]. For this reason we chose stearic acid **2a** as the first acyl donor for step 1 (*N*-acylation). Myristic acid **2b**, on the other hand, was chosen as the second acyl donor for step 2 (*O*-acylation) to mimic the structure of the sphingoid bases found in natural ceramides from human skin (18 carbons for the most common sphingoid bases) [34–37]. To achieve this, the C14 carbon chain of myristic acid **2b** was conjugated to

the C3 carbon chain of 3-amino-1,2-propanediol **1** via an ester bond, giving a chain of 18 atoms with 17 carbons and 1 oxygen.

In a preliminary study, the two reactions were conducted under stoichiometric conditions using a substrate concentration of 100 mM at a flow rate of 250 µl min^{-1} for step 1, and a substrate concentration of 50 mM at a flow rate of 125 µl min^{-1} for step 2. Two stainless steel columns, one 95 mm in length with an inner diameter of 5 mm, the other 145 mm in length with an inner diameter of 5 mm, were packed with 430 and 875 mg of Novozym® 435 to constitute the catalytic beds for steps 1 and 2, respectively. After production under these non-optimized conditions and purification, the products of each step were analyzed by IR and NMR spectroscopy. It was thus demonstrated that *N*-stearyl-3-amino-1,2-propanediol (amide **3a**) was selectively produced at step 1 with a 76 % yield and a production rate of 2.65 mmol h^{-1} $g_{biocatalyst}^{-1}$ (948 mg h^{-1} $g_{biocatalyst}^{-1}$), while 1-*O*-myristyl,3-*N*-stearyl 3-amino-1,2-propanediol (amido-ester **4**) was produced at step 2, also selectively, with a 24 % yield and a production rate of 0.1 mmol h^{-1} $g_{biocatalyst}^{-1}$ (58 mg h^{-1} $g_{biocatalyst}^{-1}$). Indeed, no secondary product was detected for both steps. These results confirmed that step 1 is exclusively chemoselective for the *N*-acylation of 3-amino-1,2-propanediol while step 2 is regioselective for the *O*-acylation of the primary alcohol function in position 1. This corroborates the results obtained in a preliminary study which demonstrated the same selectivity for the two steps of the same process performed in a batch bioreactor (data not shown). Furthermore, these results are also in agreement with data already published, regarding the Novozym® 435-catalyzed acylation of substrates structurally related to 3-amino-1,2-propanediol, carried out in similar organic solvents. These works were performed in a batch bioreactor using myristic acid as the acyl donor. First, the acylation of alaninol (2-amino-1-propanol) demonstrated the chemoselectivity for the *N*-acylation, with the production of 2-*N*-myristyl 2-amino-1-propanol only [27, 28], which is similar to the results obtained at step 1 of the continuous process.

Secondly, the *O*-acylation of 1,2-propanediol was regioselective for the primary alcohol function in position 1 [28].

All these preliminary results showed that the selectivity of both steps of the process does not need to be controlled during its implementation. Nevertheless, despite being encouraging in terms of yield and production rate, they were not satisfying enough to envisage scaling up the process. Starting from this fact, we thus concentrated our efforts on optimizing both steps of the process. For that purpose, the influences of feed flow rate, quantity of biocatalyst, substrate concentration and substrate molar ratio were examined. These parameters are likely to have a significant effect on the yield and productivity of a continuous enzymatic process.

3.1. Optimization of the process

3.1.1. Effect of feed flow rate

The feed flow rate plays an essential role in the continuous operation because it is related to the residence time of the substrates and products in the column. In order to achieve a higher synthesis yield for each step of the process, a sufficient residence time is needed to ensure that the substrate is interacting with the enzyme's active site. We thus examined the effect of feed flow rate on both synthesis yield and production rate (Fig. 2).

Fig. 2

During the first step, the flow rate was varied from 125 to 1000 µl min^{-1} (Fig. 2A). The amide **3a** yield was relatively constant and close to 80% from 125 to 500 µl min^{-1}. In parallel, the amide **3a** production rate was shown to increase to a maximum value close to 6 mmol h^{-1} $g_{biocatalyst}^{-1}$ (2145 mg h^{-1} $g_{biocatalyst}^{-1}$). On the other hand, the amide yield and production decreased to 37% and 5.2 mmol h^{-1} $g_{biocatalyst}^{-1}$ at a flow rate of 1000 µl min^{-1}. These results could be explained by the reduction in the substrate residence time within the packed-bed bioreactor, which was very likely caused by the increase in flow rate. Thus, at 1000 µl min^{-1},

the residence time was probably not sufficient for the *N*-acylation reaction to reach thermodynamic equilibrium, which resulted in a lower yield. From these results, 500 µl min^{-1} was considered as the optimum flow rate for step 1.

During the second step, the flow rate was varied from 125 to 500 µl min^{-1} (Fig. 2B). Again, a relatively constant yield of pseudo-ceramide **4** of roughly 25% was obtained using flow rates within this range, with a maximum yield of 30% at a flow rate of 250 µl min^{-1}. The reduction in the substrate residence time in the packed-bed bioreactor caused by the increase in the flow rate thus had no effect on the yield, as was already observed for the first step. In contrast, the production rate was shown to increase in conjunction with the faster flow rate, reaching a maximum value of 0.38 mmol h^{-1} $g_{biocatalyst}^{-1}$ at a flow rate of 500 µl min^{-1}. However, this flow rate gave the lowest yield (22%). For this reason 250 µl min^{-1} was taken as a compromise optimum flow rate value to achieve both the higher yield of 30% and a good production rate of 0.26 mmol h^{-1} $g_{biocatalyst}^{-1}$ (148 mg h^{-1} $g_{biocatalyst}^{-1}$) in the second step.

3.1.2. Effect of the quantity of biocatalyst

The effect of the quantity of biocatalyst on both yield and production was investigated using various quantities of Novozym® 435 packed into the packed-bed continuous reactor (Fig. 3).

Fig. 3

During the first step, the quantity of biocatalyst was varied from 215 to 1800 mg (Fig. 3A). The lowest biocatalyst quantity of 215 mg resulted in the lowest amide **3a** yield obtained in this study (17%). Starting from this value, the amide yield increased as a function of the quantity of biocatalyst rising to 87% for 875 mg of Novozym® 435. Nevertheless, when the quantity of biocatalyst was doubled (1800 mg), the amide **3a** yield did not exceed 85%. From these results, we concluded that the thermodynamic equilibrium of the reaction was already attained at 875 mg of biocatalyst. In parallel, amide **3a** production dramatically increased

within the range 215-430 mg, rising to 1.38 mmol h^{-1} $g_{biocatalyst}^{-1}$ (493 mg h^{-1} $g_{biocatalyst}^{-1}$), whereas the yield did not exceed 79% and thermodynamic equilibrium was not reached. The optimum quantity of biocatalyst for this step thus seems to be 875 mg because this represents the best compromise between a high amide yield of 87% and the low cost of Novozym® 435, despite the non-optimal production rate.

During the second step, the quantity of biocatalyst was varied from 430 to 2700 mg (Fig. 3B). There was a degree of similarity in terms of the change in both the yield and the production rate of pseudo-ceramide **4** and amide **3a**. The yield of pseudo-ceramide **4** increased to 24% when the quantity of biocatalyst was increased from 430 mg to 875 mg but it did not exceed 25% when the quantity of Novozym® 435 was doubled (1800 mg). From these results we concluded that the thermodynamic equilibrium of the reaction had already been reached at 875 mg of biocatalyst, as highlighted for the first step of *N*-acylation. In parallel, the production rate of pseudo-ceramide **4** continuously decreased as the quantity of biocatalyst was increased, falling from an initial rate of 0.18 mmol h^{-1} $g_{biocatalyst}^{-1}$ (102 mg h^{-1} $g_{biocatalyst}^{-1}$) to barely 0.02 mmol h^{-1} $g_{biocatalyst}^{-1}$ for a 16% yield with 2700 mg of Novozym® 435. This loss of both yield and productivity may be explained by the fact that step 2 of pseudo-ceramide synthesis consists in a reverse hydrolysis and is consequently accompanied by the production of water molecules that gradually accumulate in the reaction medium. So, by increasing the amount of biocatalyst, a greater quantity of synthesis product (pseudo-ceramide) and water molecules is produced which are then in contact with the biocatalyst, resulting in competition between the pseudo-ceramide hydrolysis reactions. For this reason the decrease in both the yield and the production rate of pseudo-ceramide **4**, observed when using a large quantity of immobilized lipase, may indicate that pseudo-ceramide hydrolysis is under thermodynamic control while pseudo-ceramide synthesis is under kinetic control. An increase in the quantity

of biocatalyst would then promote the thermodynamic reaction, i.e. hydrolysis, to the detriment of the synthesis.

To complete this part of the study, it is noteworthy that the optimum quantity of biocatalyst for steps 1 and 2 was 875 mg, which represented the best compromise that comprised a high synthesis yield (87% amide **3a** synthesis and 24% pseudo-ceramide **4** synthesis), an average production rate and a lower cost of Novozym® 435.

3.1.3. Effect of substrate concentration

The effect of substrate concentration on both synthesis yield and production rate was investigated using various concentrations of acyl acceptor and acyl donor under stoichiometric conditions (Fig. 4). The results could not be interpreted when the substrate concentration was higher than 100 mM due to the turbidity of the reaction mixture. This resulted in a partial solubility of the amphiphilic amide **3a** produced in step 1, or used as a substrate in step 2 in the *tert*-amyl alcohol/*n*-hexane mixture (50:50 v/v) reaction solvent. Indeed this partial substrate solubility caused plugging problems in the packed-bed bioreactor, which precluded the development of a continuous process under these conditions.

Fig. 4

The use of substrate concentrations below 100 mM during the first step appeared to have very little impact on the yield of amide **3a**, which had an average value of 82% (±5%). However, the production rate of amide **3a** significantly and continuously increased in conjunction with the increase in substrate concentration, reaching 0.75 mmol h^{-1} $g_{biocatalyst}^{-1}$ (268 mg h^{-1} $g_{biocatalyst}^{-1}$) at 100 mM of amino-diol **1** and fatty acid **2a**. Based on these results the amide production rate seemed to depend directly on the substrate concentration, while the yield was constant. Besides, 100 mM is without contest the optimum substrate concentration as it

corresponds to the highest concentration that could be used and didn't involve any problems with partial substrate solubility.

During the second step, the yield of pseudo-ceramide **4** followed a bell-shaped curve, reaching the best yield of 24% at 50 mM of substrate but decreasing to 12 and 17% for substrate concentrations of 25 and 100 mM, respectively. The decrease in yield for the lowest substrate concentrations can be explained by a dilution of the substrates in the reaction medium. The decrease in yield for the highest substrate concentrations, however, is probably due to the decrease in enzyme/substrate ratio occurring in the catalytic bed when the substrate concentration is increased. Indeed, the thermodynamic equilibrium of the reaction may not be reached if this ratio is too low, and this could lead to a decrease in yield. Furthermore, the production rate of pseudo-ceramide **4** appeared to increase from 0.02 to 0.15 mmol h^{-1} $g_{biocatalyst}^{-1}$ when the substrate concentration was increased from 25 to 75 mM. However, this rate was not enhanced by further increasing substrate concentration to 100 mM i.e. the increase in substrate concentration did not compensate for the low yield obtained at this concentration. So, in contrast to what was previously described for amide **3a** synthesis at step 1, the production rate at step 2 seems to depend on both substrate concentration and synthesis yield.

To conclude, 75 mM was the optimum substrate concentration at step 2 for the simple reason that it provided the best compromise between a pseudo-ceramide yield close to the maximum (23%) and an optimum production rate of 0.15 mmol h^{-1} $g_{biocatalyst}^{-1}$ (85 mg h^{-1} $g_{biocatalyst}^{-1}$). Nevertheless, despite the high production rate obtained, these results were not satisfying enough in terms of pseudo-ceramide yield and we consequently decided to optimize our process by varying the substrate molar ratio in order to improve the yield in step 2.

3.1.4. Effect of substrate molar ratio

399 The effect of substrate molar ratio on both the synthesis yield and the production rate of
400 pseudo-ceramide **4** (step 2) was investigated using various myristic acid **2b** concentrations
401 and a fixed *N*-stearyl 3-amino-1,2-propanediol **3a** concentration of 50 mM. The effect of
402 increasing the amide **3a** concentration was not tested due to the low solubility of this
403 compound above 50 mM and at 55°C in the *tert*-amyl alcohol/*n*-hexane mixture (50:50 v/v)
404 reaction solvent. The substrate molar ratio of fatty acid **2b** to amide **3a** was varied within the
405 range 1-5 (Fig. 5).

406 **Fig. 5**

407 Starting from values of 24% and 0.1 mmol h^{-1} $g_{biocatalyst}^{-1}$ at a molar ratio of 1, the synthesis
408 yield and production rate of pseudo-ceramide **4** were shown to increase concomitantly with
409 the molar ratio, reaching 53% and 0.22 mmol h^{-1} $g_{biocatalyst}^{-1}$ (125 mg h^{-1} $g_{biocatalyst}^{-1}$),
410 respectively, at a molar ratio of 3. This was the optimum value since a further increase in
411 substrate molar ratio led to a fall in the values of these parameters to levels close to those
412 obtained at a substrate molar ratio of 1. These results are very similar to those described by
413 Xu et al. with lipase-catalyzed interesterification reactions between triglycerides of rapeseed
414 oil and capric acid, which demonstrated that the substrate molar ratio has a double function: a
415 higher concentration of the acyl acceptor will push the reaction equilibrium toward the
416 synthesis reaction and cause an increase in the theoretical maximum product yield, whereas a
417 higher free fatty acid content will increase the possibility of an inhibition effect and require a
418 longer reaction time to reach equilibrium [38]. Nevertheless, the results are interesting since
419 the pseudo-ceramide synthesis yield was enhanced by a factor of 2 compared to all the
420 previous results, and there was no decrease in the production rate.

421 Based on these encouraging results, we tested the best operational conditions identified so far:
422 the flow rate was (only) doubled to 250 µl min^{-1}, and we chose a substrate molar ratio of

myristic acid **2b** (150 mM) to *N*-stearyl 3-amino-1,2-propanediol **3a** (50 mM) of 3, a stainless steel column 145 mm in length with a 5 mm inner diameter packed with 875 mg of Novozym® 435 to constitute the catalytic bed. Under these optimized conditions, pseudo-ceramide **4** was still produced with a yield of 54% but the production rate was doubled, reaching 0.46 mmol h^{-1} $g_{biocatalyst}^{-1}$ (261 mg h^{-1} $g_{biocatalyst}^{-1}$).

To complete the study we wanted to scale-up our process. We thus decided to test various acyl donors in the first stage to evaluate the possibility that our process could be used for the synthesis of different pseudo-ceramides. The stability of Novozym® 435, which was an essential condition prior to considering any further scale-up, was also investigated.

3.2. Scale up of the process

3.2.1. Variation of the acyl donor nature

In this part, the nature of the acyl donor was varied and evaluated at step 1 of the process. *N*-acylation of 3-amino-1,2-propanediol was thus performed to compare five acyl donors, three saturated fatty acids of various chain length (C12-C18) and two unsaturated C18 fatty acids. The conditions previously optimized in terms of feed flow rate, substrate concentration, quantity of biocatalyst and bioreactor design were used in the process. Fig. 6 shows the yields of *N*-stearyl-, *N*-myristyl-, *N*-lauryl-, *N*-oleyl- and *N*-linoleyl-3-amino-1,2-propanediol (amides **3a**, **3b**, **3c**, **3d** and **3e**, respectively) obtained after continuous Novozym®-435-catalyzed *N*-acylation of 3-amino-1,2-propanediol **1** using stearic acid **2a**, myristic acid **2b**, lauric acid **2c**, oleic acid **2d** and linoleic acid **2e** as acid donors, respectively.

Fig. 6

We observed that the yields obtained with saturated fatty acids **2a**, **2b** and **2c** ranged from 87% with lauric acid **2c** to 95% with myristic acid **2b**, which indicated that acyl chain length

had no significant effect on the amide yield. In addition, the use of unsaturated fatty acids **2d** (C18:1) and **2e** (C18:2) gave yields of 85% and 80%, respectively. These results were barely lower than the yield of 92% obtained using a saturated C18 fatty acid, stearic acid **2a**. Thus, the presence of one or two unsaturations on the carbon chain of the acyl donor did not appear to have a significant influence on the amide yield. To conclude this part of the study, an amide yield superior or equal to 80% was obtained with every fatty acid used as an acyl donor at step 1. Furthermore, this amide yield was shown to correspond to a mass production of amide that was higher than 800 mg h^{-1} g^{-1}. From these results, it would clearly be feasible to produce a range of differently functionalized pseudo-ceramides with high yields starting from any of the five fatty acids tested in order to obtain compounds with various properties and applications.

3.2.2. Stability of Novozym® 435

The operational stability of immobilized *Candida antarctica* lipase B (Novozym® 435) in the continuous packed-bed bioreactor was studied over a 3-week period, during which the continuous *N*-acylation of 3-amino-1,2-propanediol **1** was carried out using lauric acid **2c** as the acyl donor (Fig. 7).

Fig. 7

Novozym® 435 was found to be highly stable under these conditions since no decrease was observed in *N*-lauryl 3-amino-1,2-propanediol **3c** yield after twenty-two days, with an average yield of 91% ± 3%; the productivity was of the order of 113 g of amide per g of Novozym® 435. This high stability may be partly related to the reaction solvent used. Indeed, water is produced during a reverse hydrolysis reaction so controlling water activity will consequently be of great importance, especially in a continuous process. According to the literature, a polar solvent such as *tert*-amyl alcohol can be used to control water activity in a continuous

acylation process [39, 40]. The *tert*-amyl alcohol polarity would thus enable the water produced to be evacuated, resulting in a partial drying of the immobilized lipase. As a result, optimal water activity would be maintained inside the reactor and optimum enzymatic activity would remain stable for a long time.

The excellent stability of Novozym® 435 in the continuous packed-bed bioreactor allowed us to envisage further large scale pseudo-ceramide production given that the cost of the biocatalyst would not be a limiting factor.

3.2.3. Scale up of the bioreactor design

In order to perform a future scale-up of the packed-bed bioreactor to a pilot scale, the influence of reactor design on the yield and production rate of pseudo-ceramide **4** (step 2) was studied using two stainless steel columns of different geometries: column A was 125 mm in length with a 10 mm inner diameter and column B was 5 mm in length with a 50 mm inner diameter. Both columns were packed with 3300 mg of Novozym® 435 to constitute the catalytic bed, which was roughly a four-fold scale up in terms of the optimized quantity of 875 mg of biocatalyst determined at the laboratory scale. In both cases, the flow rate was varied from 100 to 1200 µl min^{-1} to change the residence time of the substrates (Fig. 8).

Fig. 8

It is interesting to note that optimum pseudo-ceramide **4** yields of close to 30% were obtained in both cases at different flow rates, depending on the type of column used. Thus, the optimal yield was obtained for column A at a flow rate of 800 µl min^{-1} (residence time of 12.5 minutes), which corresponded to the highest production of 0.23 mmol h^{-1} $g_{biocatalyst}^{-1}$ (131 mg h^{-1} $g_{biocatalyst}^{-1}$), and the optimal yield was obtained for column B at a flow rate of 200 µl min^{-1} (residence time of 50 minutes), which corresponded to a production rate of only 0.05 mmol h^{-}

493 ^{1} $g_{biocatalyst}^{-1}$ (28 mg h^{-1} $g_{biocatalyst}^{-1}$). These results demonstrate that the use of a column with a
494 large diameter and a short length, such as column B, does not improve productivity.

495 In an enzymatic packed-bed bioreactor, two transport phenomena occur. The first involves the
496 transfer of the substrate from the bulk liquid phase to the surface of the immobilized
497 biocatalyst as a result of the formation of a fictitious laminar film. The second is the
498 simultaneous diffusion of the substrate and its reaction within the biocatalyst particles.
499 Internal diffusion limitations within porous carriers indicate that the slowest step is the
500 penetration of the substrate into the interior of the catalyst particle. On the other hand,
501 external mass transfer limitations occur if the rate of transport by diffusion through the
502 laminar film is rate limiting [41]. According to the literature, external mass transfer in packed-
503 bed reactors can be improved by decreasing linear velocity, which is generally enhanced by
504 decreasing the flow rate of the substrate or by changing the column reactor length-to-diameter
505 ratio (L/d) [42–45]. In this work, for a given flow rate of 800 µl min^{-1}, linear velocity values
506 of 17 and 0.7 mm s^{-1} were obtained for columns A (L/d = 12.5) and B (L/d = 0.1),
507 respectively. Thus, the very low linear velocity obtained for column B under these conditions
508 increased the risk of external mass transfer limitation, which most likely explains the low
509 yield obtained for column B (17%) compared to column A (linear velocity 24 times higher
510 than column B). Moreover, as described above, when we used a 145 mm long column with a
511 5 mm inner diameter, the optimal yield was obtained at a flow rate of 250 µl min^{-1} (see
512 section 3.1.1), giving a linear velocity of 21 mm s^{-1}. Interestingly, this is of the same order as
513 the value obtained for column A (17 mm s^{-1}) and confirms that a high linear velocity is
514 needed to minimize external mass transfer limitation and favor synthesis.

515 These results show that it is essential to use a long column with a small diameter such as
516 column A (125 mm in length and 10 mm inner diameter) or the column used in other parts of
517 this work (145 mm in length and 5 mm inner diameter). These columns both have a L/d ratio

within the range 12.5-29, which for this reason could be taken as an optimum L/d reference range to maintain an optimum yield and productivity in our continuous process. In addition, it is also necessary to have an adequate flow rate that produces a sufficiently high linear velocity (close to 20 mm s^{-1}) to facilitate external mass transfer.

3.2.4. Economic evaluation of the process

The final objective of this work was to perform an economic evaluation of our continuous process under the optimal synthesis conditions for the two steps of the process. The economic viability of an enzymatic synthesis process is determined by several key variables including the manufacturing cost, the environmental cost, and the selling price and marketing cost for the product. The term "manufacturing cost" is used to describe the total costs involved in the manufacture of a synthetic product, which includes the cost of the biocatalyst, the chemicals, the solvents, the equipment, the energy and other operational costs. In our case, we observed the economic impact of three parameters which directly influence the manufacturing cost: the cost of the biocatalyst, the substrates and the organic solvents (reaction solvents and solvents used for the purification of the synthesis products).

In order to achieve a better assessment of the economic cost, we drew up a balance sheet of the two steps of the process. Under our optimized experimental conditions used at a 4-fold scale-up, an amide yield of 90% and a production rate of 1821 mg h^{-1} were obtained at step 1 (*N*-acylation) using 3300 mg of biocatalyst packed into the bioreactor. Assuming a biocatalyst lifespan of 3 weeks, a productivity of 918 g amide was obtained. Similarly, for step 2 (*O*-acylation), a pseudo-ceramide yield of 30% and a production rate of 432 mg h^{-1} were obtained (see section 3.2.3), which corresponds to a productivity of 218 g of pseudo-ceramide. To evaluate the cost effectiveness of the proposed process, the cost of pseudo-ceramide production was calculated by considering the second step as the limiting step of the process in

terms of production and yield. So, given the price of the biocatalyst (Novozym® 435), the substrates (3-amino-1,2-propanediol **1**, stearic acid **2a** and myristic acid **2b**) and the solvents (*tert*-amyl alcohol, *n*-hexane and purification solvents), we calculated the cost of producing one kg of pseudo-ceramide under our optimal conditions: 21 € of biocatalyst, 351 € of substrates and 1,422 € of organic solvents. Suppliers quoted prices of about 2000 €/kg for the cheapest synthetic ceramide compounds. In consequence, the cost of the biocatalyst, substrates and organic solvents represent 1%, 18% and 71% of the product price, respectively. The cost of the biocatalyst is usually one of the essential factors of the economic cost of an enzymatic synthesis process due to the high price of biocatalysts (Novozym® 435: 1100 €/kg). However, it is noteworthy that the pseudo-ceramide productivity of our continuous process in packed-bed bioreactor (69 $g_{pseudo\text{-}ceramide}\ g_{biocatalyst}^{-1}$) was approximately 5-fold higher than the results obtained in a process already developed for the synthesis of pseudo-ceramides in a batch bioreactor (15 $g_{pseudo\text{-}ceramide}\ g_{biocatalyst}^{-1}$) [26], which shows that this method greatly reduces the economic cost of the biocatalyst. These results are thus encouraging in terms of the future development of this continuous process on a pilot scale but also demonstrate the need to recover and reuse the organic solvents as this could potentially have a significant impact on the cost effectiveness. Moreover, the production of pseudo-ceramides with a purity close to 99%, like some commercial ceramides, would require the development of a purification method applicable on a large scale, such as liquid extraction or low pressure liquid chromatography.

4. Conclusion

In this work, we developed a new efficient continuous process for the selective Novozym® 435-catalyzed synthesis of pseudo-ceramides, conducted in a packed-bed bioreactor. To our knowledge, only batch bioreactors had indeed been used so far to develop the lipase-catalyzed synthesis of pseudo-ceramides or ceramides [11-13, 27]. Our process involved two steps for

the optimization of the selective diacylation of 3-amino-1,2-propanediol **1** conducted in a *tert*-amyl alcohol/*n*-hexane mixture (50:50 v/v), starting from two fatty acids as acyl donors: stearic acid **2a** (step 1) and myristic acid **2b** (step 2).

During the first step, the *N*-acylation of 3-amino-1,2-propanediol **1**, the operational conditions of flow rate, quantity of biocatalyst and substrate concentration were optimized and an excellent synthesis yield of 92%, associated with a very good production rate of 3.15 mmol h^{-1} $g_{biocatalyst}^{-1}$ (1128 mg h^{-1} $g_{biocatalyst}^{-1}$) were obtained. During the second step, which involved the *O*-acylation of the *N*-stearyl 3-amino-1,2-propanediol **3a** produced in the first step, we optimized the same operational conditions as in the first step together with the substrate molar ratio. Under the best conditions identified, the desired pseudo-ceramide, i.e. 1-*O*-myristyl,3-*N*-stearyl 3-amino-1,2-propanediol **4**, was produced at a satisfying yield of 54% and a production rate of 0.46 mmol h^{-1} $g_{biocatalyst}^{-1}$ (261 mg h^{-1} $g_{biocatalyst}^{-1}$).

These results clearly demonstrate that this two-step process has great potential for the industrial scale production of *N,O*-diacyl 3-amino-1,2-propanediol-type pseudo-ceramides, and in particular the 1-*O*-myristyl,3-*N*-stearyl 3-amino-1,2-propanediol **4** synthesized in this work. This assumption is first strengthened by the fact that the productivity of pseudo-ceramide synthesis for this process was approximately improved by a factor 5, compared to the results obtained in a process already developed in a batch bioreactor [26]. On the other hand, we have shown that various fatty acids could be used as acyl donors in step 1 of our process, so its use for the synthesis of different pseudo-ceramides can be seriously envisaged.

Finally, in order to better assess the economic cost of pseudo-ceramide production we drew up a balance sheet of the two steps of the process at a 4-fold scale-up. So, given the suppliers' quoted prices of about 2000 €/kg for the cheapest synthetic ceramide compounds, the cost of the biocatalyst, substrates and organic solvents used for synthesis and purification represented 1%, 18% and 71% of the product price, respectively. These results are encouraging in terms

592 of the future development of this continuous process on a pilot scale, especially at the level of
593 the cost of the biocatalyst (Novozym® 435 can operate for more than 3 weeks without a drop
594 in yield during step 1). But they also demonstrate the need to recover and reuse the organic
595 solvents and to work on the development of the purification process as this could potentially
596 have a significant impact on the cost effectiveness.

Acknowledgments

This study was supported by the Centre National de la Recherche Scientifique and the French ANR (National Research Agency) through the EXPENANTIO project (CP2P program: Chimie et Procédés pour le Développement Durable).

References

[1] L. Coderch, O. López, A. de la Maza, J.L. Parra, Am. J. Clin. Dermatol. 2 (2003) 107–129.

[2] M. Kerscher, H.C. Korting, M. Schäfer-Korting, Eur. J. Dermatol. 1 (1991) 39–43.

[3] M. Fillet, M. Bentires-Alj, V. Deregowski, R. Greimers, J. Gielen, J. Piette, V. Bours, M.-P. Merville, Biochem. Pharmacol. 10 (2003) 1633–1642.

[4] H. Garg, N. Francella, K.A. Tony, L.A. Augustine, J.J. Barchi Jr, J. Fantini, A. Puri, D.R. Mootoo, R. Blumenthal, Antiviral Res. 1 (2008) 54–61.

[5] J.-F. Molina, Househ. Pers. Care Today. (2008) 12–15.

[6] S.H. Cho, L.J. Frew, P. Chandar, S.A. Madison, US Patent 5,476,671 A (1995).

[7] M. Philippe, D. Semeria, European Patent 884,305 A1 (1998).

[8] J.W.H. Smeets, P.G. Weber, US Patent 5,631,356 A (1997).

[9] H.-J. Ha, M.C. Hong, S.W. Ko, Y.W. Kim, W.K. Lee, J. Park, Bioorg. Med. Chem. Lett. 7 (2006) 1880–1883.

[10] E. Rochlin, US Patent CA2,373,286A1 (2000).

[11] M. Bakke, M. Takizawa, T. Sugai, H. Ohta, J. Org. Chem. 20 (1998) 6929–6938.

[12] L. Couturier, D. Taupin, F. Yvergnaux, J. Mol. Catal. B Enzym. 1 (2009) 29–33.

[13] R.M. De Pater, J.W.J. Lambers, J.W.H. Smeets, US Patent 561,004,0 A (1997).

[14] M.J. Haas, P.S. Fox, T.A. Foglia, Eur. J. Lipid Sci. Technol. 2 (2011) 168–179.

[15] M. Kapoor, M.N. Gupta, Process Biochem. 4 (2012) 555–569.

[16] B.M. Nestl, B.A. Nebel, B. Hauer, Curr. Opin. Chem. Biol. 2 (2011) 187–193.

[17] D. Sharma, B. Sharma, A.K. Shukla, Biotechnology. 1 (2011) 23–40.

[18] A. Tomin, G. Hornyánszky, K. Kupai, Z. Dorkó, L. Ürge, F. Darvas, L. Poppe, Process Biochem. 6 (2010) 859–865.

[19] N. Doukyu, H. Ogino, Biochem. Eng. J. 3 (2010) 270–282.

627 [20] M. Fernández-Pérez, C. Otero, Enzyme Microb. Technol. 6 (2001) 527–536.
628 [21] M. Fernández-Pérez, C. Otero, Enzyme Microb. Technol. 5 (2003) 650–660.
629 [22] T. Furutani, M. Furui, H. Ooshima, J. Kato, Enzyme Microb. Technol. 8 (1996) 578–
630 584.
631 [23] V. Gotor, R. Brieva, F. Rebolledo, J. Chem. Soc. Chem. Commun. 14 (1988) 957–
632 958.
633 [24] L.T. Kanerva, M. Kosonen, E. Vänttinen, T.T. Huuhtanen, M. Dahlqvist, M.M. Kady,
634 S.B. Christensen, Acta Chem. Scand. 11 (1992) 1101–1105.
635 [25] O. Torre, V. Gotor-Fernández, V. Gotor, Tetrahedron Asymmetry. 5 (2006) 860–866.
636 [26] L. Lassalle, F. Yvergnaux, European Patent 20,040,767,243 (2008).
637 [27] F. Le Joubioux, Y. Ben Henda, N. Bridiau, O. Achour, M. Graber, T. Maugard, J.
638 Mol. Catal. B Enzym. 85-86 (2013) 193–199.
639 [28] P.O. Syren, F. Le Joubioux, Y. Ben Henda, T. Maugard, K. Hult, M. Graber, Chem.
640 Cat. Chem. 5 (2013) 1842–1853.
641 [29] T. Takanami, H. Tokoro, D. Kato, S. Nishiyama, T. Sugai, Tetrahedron Lett. 46
642 (2005) 3291-3295.
643 [30] S.-W. Chang, J.-F. Shaw, C.-K. Yang, C.-J. Shieh, Process Biochem. 9 (2007) 1362–
644 1366.
645 [31] A. H-Kittikun, W. Kaewthong, B. Cheirsilp, Biochem. Eng. J. 1 (2008) 116–120.
646 [32] L. Couturier, F. Yvergnaux, Int. J. Cosmetic Sci. 31 (2009) 209-224.
647 [33] F. Le Joubioux, N. Bridiau, Y. Ben Henda, O. Achour, M. Graber, T. Maugard, J.
648 Mol. Catal. B Enzym. (2013) 99–110.
649 [34] C. Bijani, PhD Thesis, 2010.
650 [35] R. Schnaar, A. Suzuki, P. Stanley, in: A. Varki, R.D. Cummings, J.D. Esko, H.H.
651 Freeze, P. Stanley, C.R. Bertozzi, G.W. Hart, M.E. Etzler (Eds.), Essentials of

652 Glycobiology, 2nd edition, Cold Spring Harbor Laboratory Press. New York, 2009, pp.
653 129–142.
654 [36] P.W. Wertz, M.C. Miethke, S.A. Long, J.S. Strauss, D.T. Downing, J. Invest.
655 Dermatol. 5 (1985) 410–412.
656 [37] W. Zheng, J. Kollmeyer, H. Symolon, A. Momin, E. Munter, E. Wang, S. Kelly, J.C.
657 Allegood, Y. Liu, Q. Peng, H. Ramaraju, M.C. Sullards, M. Cabot, A.H. Merrill Jr,
658 Biochim. Biophys. Acta. 12 (2006) 1864–1884.
659 [38] X. Xu, S. Balchen, C.-E. Høy, J. Adler-Nissen, J Am Oil Chem Soc. (1998) 1573–
660 1579.
661 [39] S. Colombié, R.J. Tweddell, J.S. Condoret, A. Marty, Biotechnol. Bioeng. 3 (1998)
662 362–368.
663 [40] W.F. Slotema, G. Sandoval, D. Guieysse, A.J.J. Straathof, A. Marty, Biotechnol.
664 Bioeng. 6 (2003) 664–669.
665 [41] Y.H. Chew, C.T. Lee, M.R. Sarmidi, R.A. Aziz, F. Razali, Food Bioprod. Process. 4
666 (2008) 276–282.
667 [42] A.P. Ison, A.R. Macrae, C.G. Smith, J. Bosley, Biotechnol. Bioeng. 2 (1994) 122–130.
668 [43] Y. Iwasaki, T. Yamane, in: H.W. Gardner and T.M. Kuo (Eds.), Lipid biotechnology,
669 Marcel Dekker, Inc. New York, 2002, pp. 421–422.
670 [44] M. Linde Damstrup, PhD Thesis, 2008.
671 [45] E. Szomanski, Proc. Third Australas. Conf. Hydraul. Fluid Mech. (1970) 117–123.
672
673

Scheme 1. Two-step process for the selective enzymatic synthesis of 1-*O*,3-*N*-diacyl 3-amino-1,2-propanediol-type pseudo-ceramides catalyzed by Novozym® 435 in a packed-bed bioreactor.

Fig. 1. Experimental setup for the continuous Novozym® 435-catalyzed acylation reaction conducted in a packed-bed bioreactor system.

Fig. 2. Effect of flow rate on the synthesis yield (△) and production rate (●) of **amide 3a (step 1, A)** and **pseudo-ceramide 4 (step 2, B)**. The reactions were carried out at 55°C in a *tert*-amyl alcohol/*n*-hexane mixture (50:50 v/v) using substrate concentrations of 100 (**A**: amino-diol **1** and stearic acid **2a**) and 50 mM (**B**: amide **3a** and myristic acid **2b**) under stoichiometric conditions. Stainless steel columns 95 mm in length with an inner diameter of 5 mm (**A**), and 145 mm in length with a 5 mm inner diameter (**B**), were packed with 430 (**A**) and 875 mg (**B**) of Novozym® 435 to constitute the catalytic beds.

Fig. 3. Effect of the quantity of biocatalyst on the synthesis yield (△) and production rate (●) of **amide 3a (step 1, A)** and **pseudo-ceramide 4 (step 2, B)**. The reactions were carried out at 55°C in a *tert*-amyl alcohol/*n*-hexane mixture (50:50 v/v), at a flow rate of 125 µl min^{-1} and substrate concentrations of 100 (**A**: amino-diol **1** and stearic acid **2a**) and 50 mM (**B**: amide **3a** and myristic acid **2b**) under stoichiometric conditions. Stainless steel columns with an inner diameter of 5 mm and of variable length, in which various quantities of Novozym® 435 could be packed, were used as the catalytic beds.

Fig. 4. Effect of substrate concentration on the synthesis yield (△) and production rate (●) of **amide 3a (step 1, A)** and **pseudo-ceramide 4 (step 2, B)**. The reactions were carried out at 55°C in a *tert*-amyl alcohol/*n*-hexane mixture (50:50 v/v) at a flow rate of 125 µl min^{-1} and

various substrate concentrations, from 10 to 100 mM, under stoichiometric conditions (**A**: amino-diol **1** and stearic acid **2a**; **B**: amide **3a** and myristic acid **2b**). A stainless steel column 145 mm in length with an inner diameter of 5 mm was packed with 875 mg of Novozym® 435 to constitute the catalytic bed.

Fig. 5. Effect of substrate molar ratio on the synthesis yield (△) and production rate (●) of **pseudo-ceramide 4 (step 2)**. The reactions were carried out at 55°C in a *tert*-amyl alcohol/*n*-hexane mixture (50:50 v/v) at a flow rate of 125 µl min^{-1}, various substrate molar ratios from 1 to 5 and a fixed amide **3a** concentration of 50 mM. A stainless steel column 145 mm in length with an inner diameter of 5 mm was packed with 875 mg of Novozym® 435 to constitute the catalytic bed.

Fig. 6. Effect of the nature of the fatty acid used as an acyl donor on the synthesis yield (histogram) and production rate (●) of the **amide (step 1)**, using 3-amino-1,2-propanediol **1** as the acyl acceptor and various fatty acids as acyl donors. The reactions were carried out at 55°C in a *tert*-amyl alcohol/*n*-hexane mixture (50:50 v/v) at a flow rate of 500 µl min^{-1} and a substrate concentration of 100 mM, under stoichiometric conditions. A stainless steel column 145 mm in length with an inner diameter of 5 mm was packed with 875 mg of Novozym® 435 to constitute the catalytic bed.

Fig. 7. Continuous Novozym® 435-catalyzed synthesis of **amide 3c (step 1)** over a 3 week period using 3-amino-1,2-propanediol **1** as the acyl acceptor and lauric acid **2c** as the acyl donor. The reaction was carried out at 55°C in a *tert*-amyl alcohol/*n*-hexane mixture (50:50 v/v), at a flow rate of 250 µl min^{-1} and a substrate concentration of 50 mM, under stoichiometric conditions. A stainless steel column 145 mm in length with an inner diameter of 5 mm was packed with 875 mg of Novozym® 435 to constitute the catalytic bed.

720 **Fig. 8.** Effect of reactor design on the synthesis yield (△) and production rate (●) of **pseudo-**
721 **ceramide 4 (step 2)** using column A (125 mm in length and 10 mm inner diameter) or
722 column B (5 mm in length and 50 mm inner diameter). The reactions were carried out at 55°C
723 in a *tert*-amyl alcohol/*n*-hexane mixture (50:50 v/v) with 150 mM myristic acid **2b** and 50
724 mM amide **3a**. Stainless steel columns 125 mm in length with a 10 mm inner diameter (**A**)
725 and 5 mm in length with a 50 mm inner diameter (**B**) were packed with 3300 mg of
726 Novozym® 435 to constitute the catalytic beds.

727

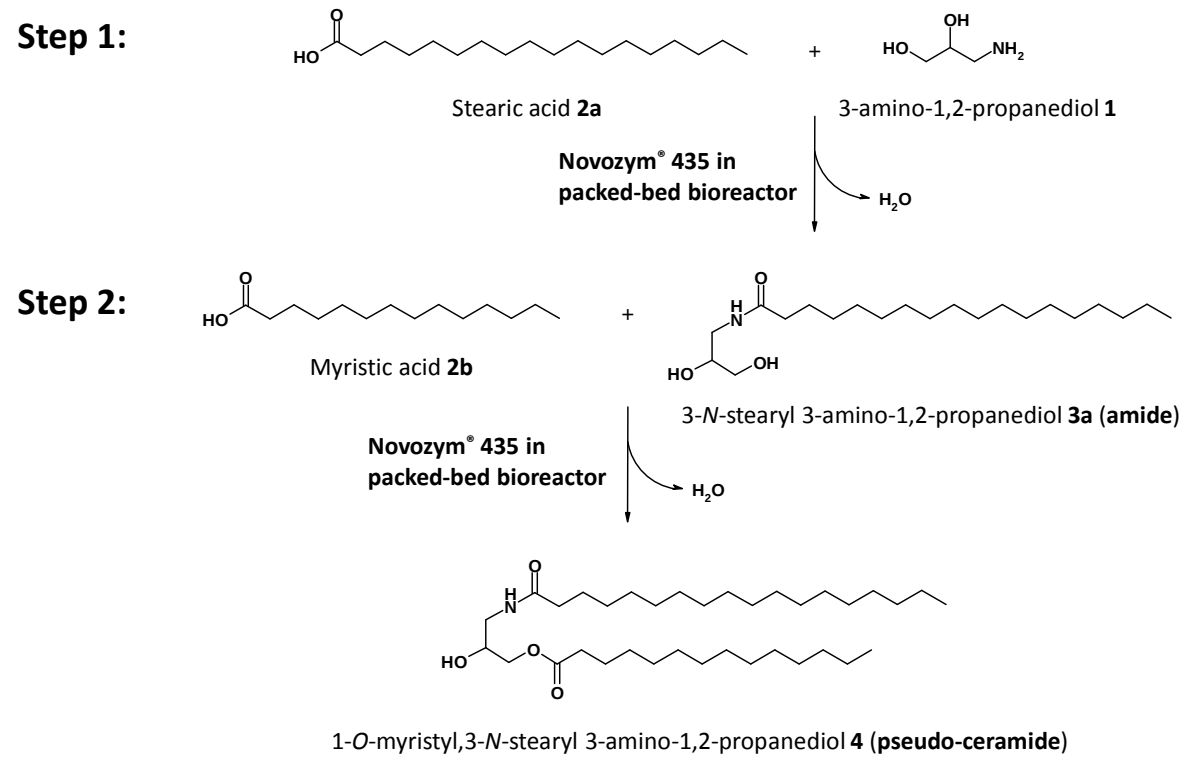

728

729 **Scheme 1.**

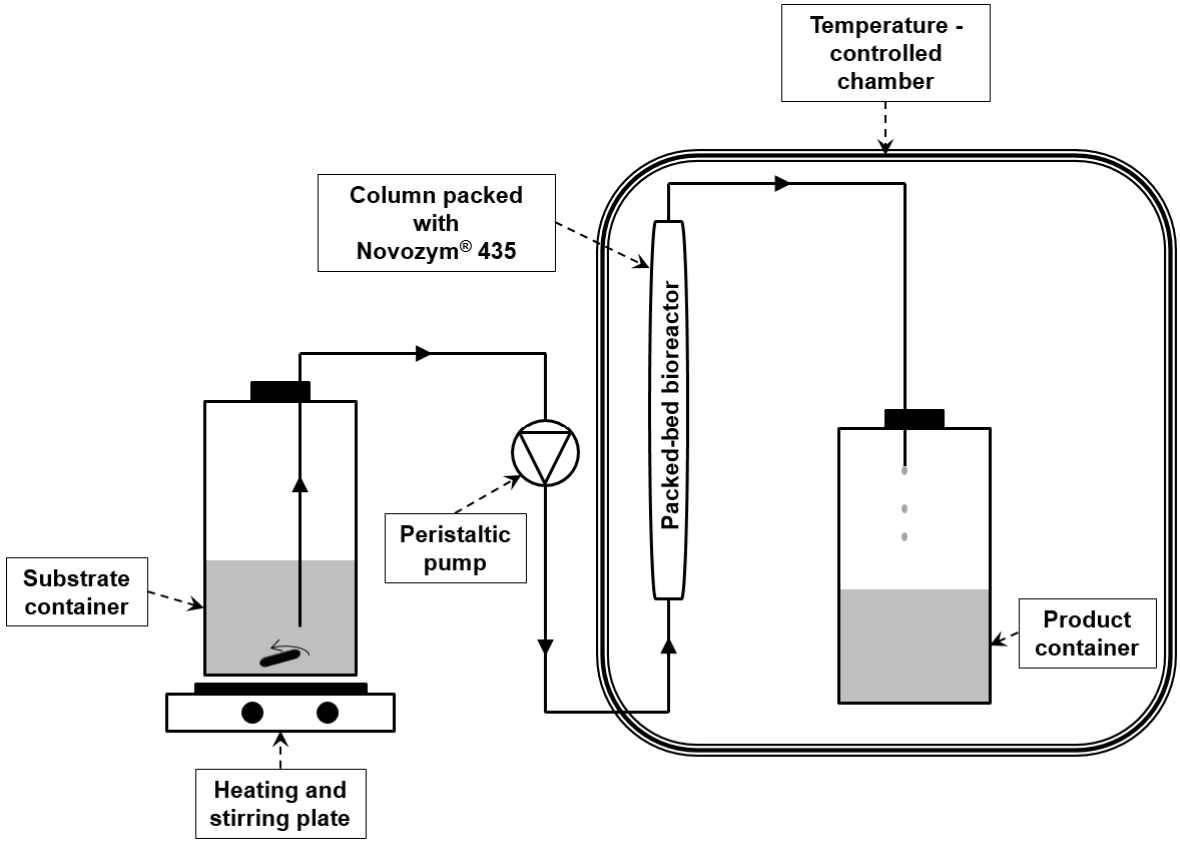
Temperature - controlled chamber
Column packed with Novozym® 435
Packed-bed bioreactor
Peristaltic pump
Substrate container
Product container
Heating and stirring plate

730

731 **Fig. 1.**

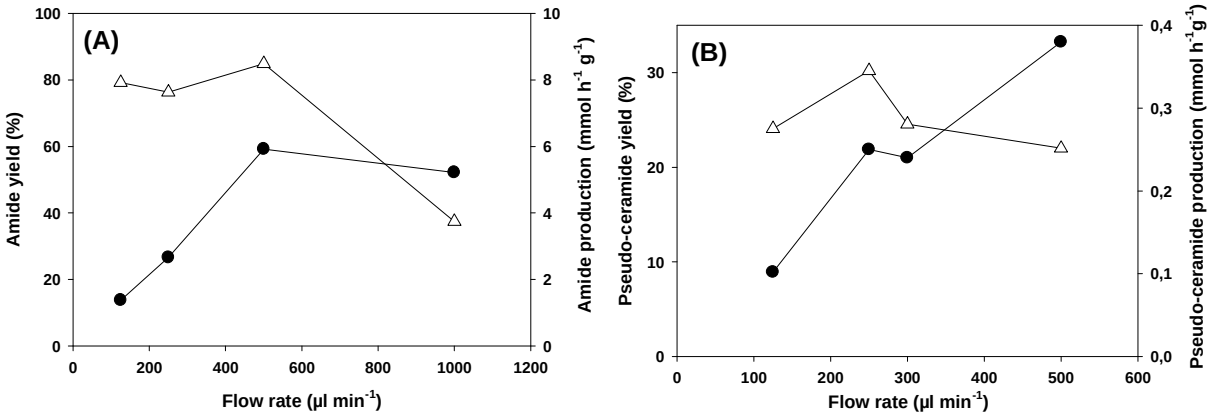
(A)
Amide yield (%)
Amide production (mmol h-1 g-1)
Flow rate (µl min-1)
(B)
Pseudo-ceramide yield (%)
Pseudo-ceramide production (mmol h-1 g-1)
Flow rate (µl min-1)

732
733 **Fig. 2.**

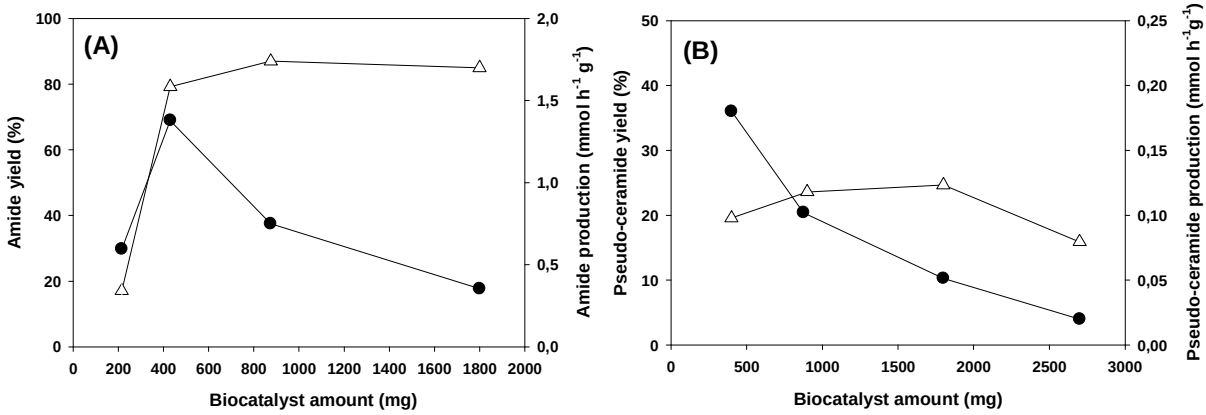
(A)
Amide yield (%)
Amide production (mmol h-1 g-1)
Biocatalyst amount (mg)
(B)
Pseudo-ceramide yield (%)
Pseudo-ceramide production (mmol h-1 g-1)
Biocatalyst amount (mg)

734

735 **Fig. 3.**

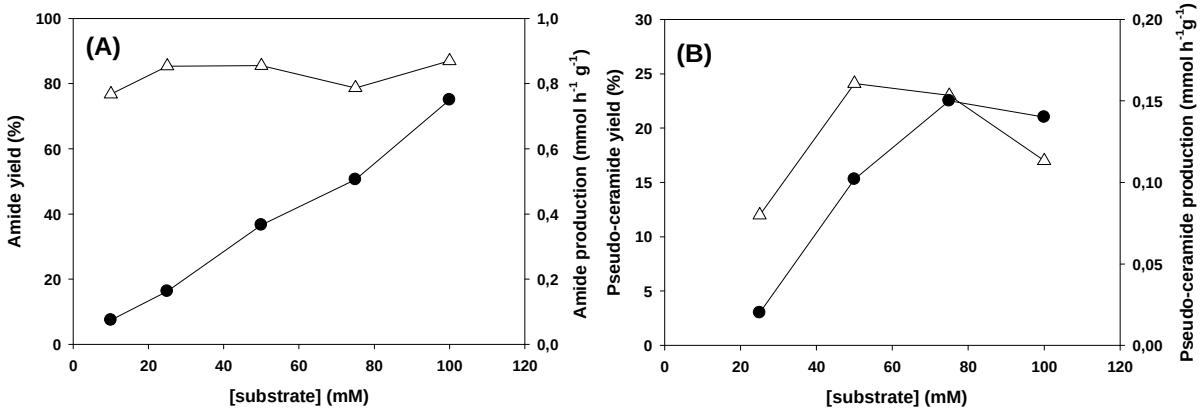
(A)
Amide yield (%)
Amide production (mmol h-1 g-1)
[substrate] (mM)
(B)
Pseudo-ceramide yield (%)
Pseudo-ceramide production (mmol h-1 g-1)
[substrate] (mM)

736

737 **Fig. 4.**

738

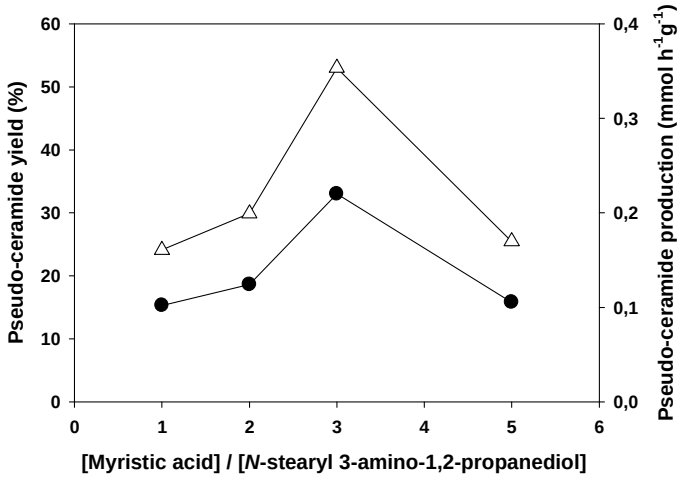
Pseudo-ceramide yield (%)
Pseudo-ceramide production (mmol h-1g-1)
[Myristic acid] / [N-stearyl 3-amino-1,2-propanediol]
0
10
20
30
40
50
60
0,0
0,1
0,2
0,3
0,4
0
1
2
3
4
5
6

739 **Fig. 5.**

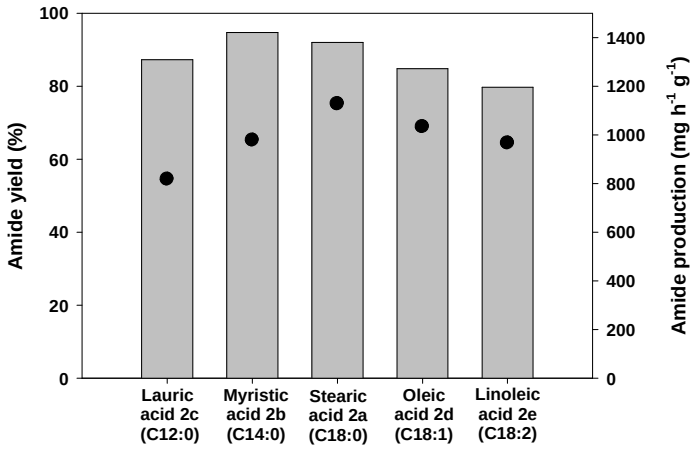
Amide yield (%)
Amide production (mg h-1 g-1)
0
20
40
60
80
100
0
200
400
600
800
1000
1200
1400
Lauric acid 2c (C12:0)
Myristic acid 2b (C14:0)
Stearic acid 2a (C18:0)
Oleic acid 2d (C18:1)
Linoleic acid 2e (C18:2)

740

741 **Fig. 6.**

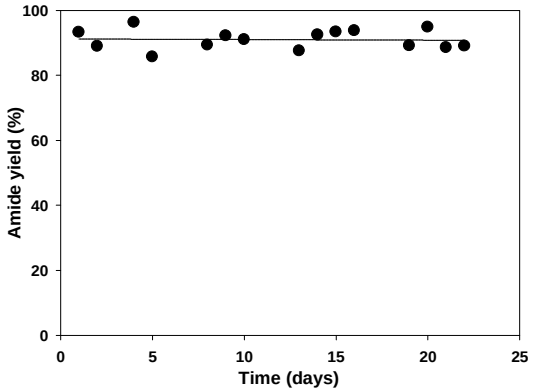

742

743 **Fig. 7.**

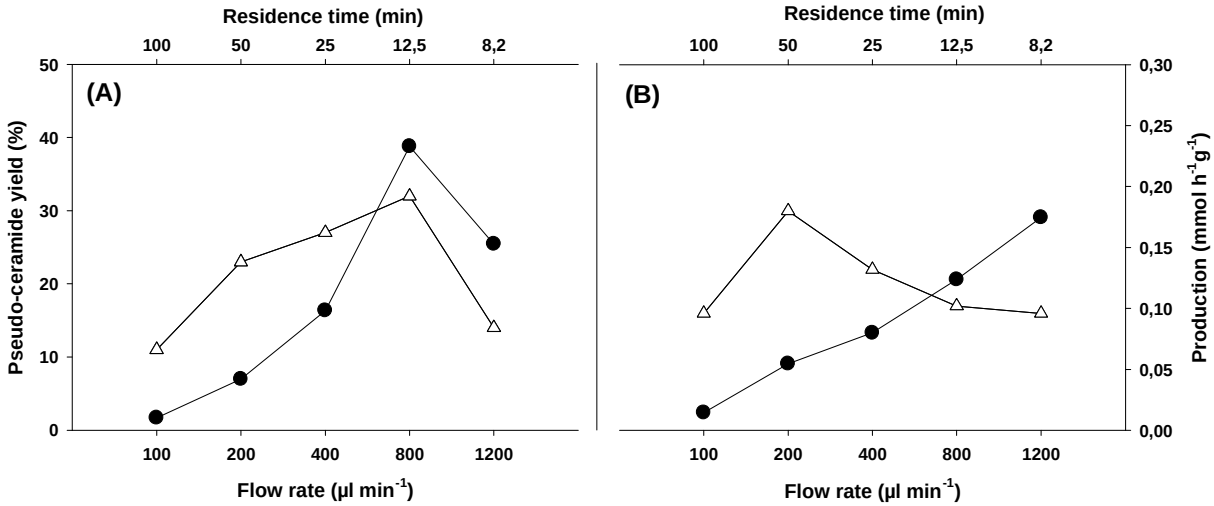

744
745 **Fig. 8.**

746

747

748 **Table 1**

749 Elution gradient for HPLC analysis

Time (min)	Solvent A: acetonitrile/water/acetic acid (77:23:0.1 v/v/v) (%)	Solvent B: methanol/acetic acid (100:0.1 v/v) (%)
0	100	0
90	100	0
93	0	100
143	0	100
145	100	0
153	100	0

750

751